1996ApJ...470...38L

THE ASTROPHYSICAL JOURNAL, 470:38–42, 1996 October 10
© 1996. The American Astronomical Society. All rights reserved. Printed in U.S.A.

THE DIPOLE OBSERVED IN THE *COBE* DMR 4 YEAR DATA

C. H. LINEWEAVER,[1,2] L. TENORIO,[3] G. F. SMOOT,[4] P. KEEGSTRA,[5] A. J. BANDAY,[5,6] AND P. LUBIN[7]

Received 1996 January 22; accepted 1996 April 30

ABSTRACT

The largest anisotropy in the cosmic microwave background (CMB) is the ≈ 3 mK dipole assumed to be due to our velocity with respect to the CMB. Using the 4 year data set from all six channels of the *COBE* Differential Microwave Radiometers (DMR), we obtain a best-fit dipole amplitude $3.358 \pm 0.001 \pm 0.023$ mK in the direction $(l, b) = (264.^\circ31 \pm 0.^\circ04 \pm 0.^\circ16, +48.^\circ05 \pm 0.^\circ02 \pm 0.^\circ09)$, where the first uncertainties are statistical and the second include calibration and combined systematic uncertainties. This measurement is consistent with previous DMR and FIRAS results.

Subject headings: cosmic microwave background — cosmology: observations

1. INTRODUCTION

The Sun's motion with respect to the cosmic microwave background (CMB) is believed to be responsible for the largest anisotropy seen in the *COBE* DMR maps: the ≈ 3 mK dipole in the direction of the constellation Leo. A measurement of this Doppler dipole thus tells us our velocity with respect to the rest frame of the CMB. A high precision measurement of the dipole will be used as the primary calibrator for an increasing number of ground, balloon, and satellite anisotropy experiments (Bersanelli et al. 1996). The accurate removal of the Doppler dipole and Doppler quadrupole from anisotropy maps improves the precision of the anisotropy results. The CMB dipole is also used to calibrate bulk flow observations, which yield independent but much less precise dipole values. In addition, anisotropy measurements in other background radiations will be made in the future and an eventual test of the Doppler origin of the CMB dipole will be facilitated by a CMB dipole of maximum precision (Lineweaver et al. 1995). In this paper we use the DMR 4 year data to determine the precise direction and the amplitude of the observed dipole. The largest source of directional error (aliasing of CMB power combined with instrument noise) has been reduced by using relatively small Galactic plane cuts.

In § 2 we discuss the data analysis, and in § 3 we discuss contamination from Galactic emission as well as other factors contributing to the error budget. In § 4 we present our results. We then discuss and compare our results to FIRAS and other reported DMR dipole results.

2. DATA ANALYSIS

The 4 year DMR data set and its systematic errors and calibration procedures are described in Kogut et al. (1996b). There are two independent channels at each of the three frequencies 31.5, 53, and 90 GHz. We base our results on all six DMR channels since the less sensitive 31 GHz channels provide useful information on the frequency dependence of Galactic contamination.

We use three methods to obtain the CMB dipole amplitude and direction. These methods differ in the form of the input data but all of them are least-squares fits of the data to the coefficients of a spherical harmonic decomposition of the sky: $T(\theta, \phi) = \sum_{lm} a_{lm} Y_{lm}(\theta, \phi)$, where the Y_{lm} are real-valued spherical harmonics as described in Smoot et al. (1991) and the dipole vector is $\boldsymbol{D} = (3/4\pi)^{1/2}(-a_{1,1}, -a_{-1,1}, a_{1,0})$. To obtain the dipole we minimize the three quantities:

$$\sum_i \left\{ T_i - \sum_{l=0}^{l_{\max}} \sum_{m=-l}^{+l} a_{lm} Y_{lm}(i) \right\}^2 \Big/ \sigma_i^2 , \quad (1)$$

$$\sum_t \left\{ \Delta T(t) - \sum_{l=0}^{l_{\max}} \sum_{m=-l}^{+l} a_{lm} [Y_{lm}(t_+) - Y_{lm}(t_-)] \right\}^2 \Big/ \sigma_t^2 , \quad (2)$$

$$\sum_{i,j>i} \left\{ \Delta T_{ij} - \sum_{l=0}^{l_{\max}} \sum_{m=-l}^{+l} a_{lm} [Y_{lm}(i) - Y_{lm}(j)] \right\}^2 \Big/ \sigma_{ij}^2 , \quad (3)$$

where T_i is a pixelized DMR temperature map, $\Delta T(t)$ is a single DMR differential measurement, and $Y_{lm}(t_+)$ and $Y_{lm}(t_-)$ are the spherical harmonics evaluated in the pointing directions of the DMR "+" and "−" horns, respectively, at time t. The pixel-pair data, ΔT_{ij}, is the average over all single measurements $\Delta T(t)$, where the antennas are pointing at pixels i and j. The denominators are the variances of the input data.

Thus, with method 1, the sum is over all map pixels, with method 2, the sum is over all the time-ordered data (with no pixelization), and in method 3 the sum is over all pixel pairs.

The three methods are consistent and agree to within the relatively small noise-only error bars for each channel. We use the difference between the nonpixelized method and the mean of the two pixelized methods to estimate and correct for the smoothing due to data pixelization.

We adopt the mean of these three methods and include the difference in the combined systematic uncertainty. We correct for beam smoothing by multiplying the amplitude by the factor 1.005 (Wright et al. 1994).

3. ANALYSIS OF GALACTIC PLANE CUTS

3.1. *Galactic Contamination*

We estimate the influence of Galactic emission on the measurement by solving for the dipoles in equations (1), (2),

[1] Observatoire de Strasbourg, 67000 Strasbourg, France.
[2] charley@cdsxb6.u-strasbg.fr.
[3] Universidad Carlos III, Madrid, Spain.
[4] Lawrence Berkeley Laboratory, Space Sciences Laboratory, and Center for Particle Astrophysics, Building 50-205, University of California, Berkeley, CA 94720.
[5] Hughes STX Corporation, Laboratory for Astronomy and Solar Physics, Code 685, NASA/Goddard Space Flight Center, Greenbelt, MD 20771.
[6] Max Planck Institut für Astrophysik, 85740, Garching, Germany.
[7] University of California Santa Barbara Physics Department, Santa Barbara, CA 93106.

© American Astronomical Society • Provided by the NASA Astrophysics Data System

1996ApJ...470...38L

and (3) for a series of Galactic plane latitude cuts. The dipole amplitude and direction results from each channel and each Galactic plane cut are shown in Figure 1.

Galactic emission produces a dipole that pulls the solutions toward it. This is easily seen in Figure 1 from the locations of the 0° and 5° cut solutions relative to the cluster of higher cut results on the right. Since the Galactic dipole vector is nearly orthogonal to the CMB dipole vector, it is almost maximally effective in influencing the CMB dipole direction and almost minimally effective in influencing the CMB dipole amplitude.

We can get a rough estimate of the Galactic dipoles by noting that the 0° cut solutions for 31, 53, and 90 GHz are displaced from the direction of our best-fit CMB dipole by angles $\alpha_\nu \approx 5°$, 1°, and 0°.5, respectively. Thus, the ratios of the Galactic dipoles to the CMB dipole are $D_{\mathrm{Gal},\nu}/D_{\mathrm{CMB}} \approx \sin(\alpha_\nu) \approx (9\%, 2\%, 1\%)$. In Figure 1, the general increase of the dipole amplitudes seen in the top panel as the Galactic cut increases from 0° to 5° to 10° can be explained by the fact that the Galactic dipole vector contains a component in the direction opposite to the CMB dipole (the Galactic center is ≈94° away) and thus reduces the total dipole in the maps. A rough estimate of this effect on the dipole solutions D is in good agreement with the plot: $\Delta D_\nu \sim \sin(4°) \sin(\alpha_\nu) D \sim (20, 5, 2\ \mu\mathrm{K})$ for 31, 53, and 90 GHz, respectively.

Figure 1 clearly shows the influence of the Galaxy for the 0° and 5° cuts as well as the relative agreement of the independent channel results for both amplitude and direction. It is also apparent that to first approximation a 10° cut is sufficient to remove the effect of the Galaxy on the direction of the best-fit dipole; increases of the cut from 10° to 15° and so on, do not push the directions away from the Galactic center or in any other particular direction. The results tend to cluster together. The directional precision of the various channels and Galactic cuts is seen to be ∼0°.3, and it is perhaps reassuring to note that at the bottom and the top of the cluster are the least sensitive 31A and 31B solutions.

Figure 2 minimizes the confusion of taking a closer look at the cluster of points in Figure 1. It analyzes the directional changes of the dipoles in the bottom panel of Figure 1. For example, consider the 31A results. The angular difference between the 5° and 10° cut solutions is a vector of length ≈1° starting from the 5° cut on the left and extending to the 10° cut on the right. Averaging this vector with the analogous vector from 31B, we obtain the long thin line that runs across most of the lower panel in Figure 2. The size of this angular deviation (≈1°) is plotted as the triangular point in the 5–10 bin of the top panel. An analogous procedure was followed for all channels and Galactic cuts. Figure 2 is thus a spectral analysis of the angular deviations from one Galactic plane cut to another.

Galactic emission significant enough to affect the dipole results will tend to pull the three channels in approximately the same direction and favor a spectral behavior typical of synchrotron or free-free emission. In the top panel of Figure 2, the two reference lines originating on the 31 GHz point in the 0–5 and 5–10 bins indicate this expected spectral behavior for synchrotron radiation (*thin lines*) and free-free emission (*thick lines*). The results in the 0–5 and 5–10 bins are obviously from Galactic emission. The directions in these bins are also strongly correlated. The absence of this spectral and directional behavior for the bins 10–15 and larger is evidence that the Galaxy is no longer the major contributor to the directional uncertainty of the dipole. Although the 20–25 bin seems indicative of the spectral behavior of Galactic emission, the incoherent directional behavior is inconsistent with a common spatial origin for the supposed source.

Evidence supporting the idea that Galactic emission is relatively unimportant is provided by the small differences between the dipole solutions using the "custom" cut (Fig. 1 of Kogut et al. 1996a) and the straight $|b| > 20°$ cut presented here. The differences in amplitude, longitude, and latitude are less than 0.2%, 9%, and 6% of our error bars on these respective quantities. If plotted in Figure 1, the "custom" cut solutions overlap the $|b| > 20°$ points with a barely distinguishable displacement in the direction of the $|b| > 25°$ solutions.

3.2. *Higher Multipole CMB Contamination*

For the purposes of determining the dipole there are two sources of noise; instrument noise with a power-law spectral index $n \approx 3$ and the $n \approx 1$ CMB signal. At 10° scales the CMB signal to noise ratio in the maps is ∼2 (Bennett et al. 1996). Thus, on larger scales the CMB signal dominates the instrument noise, and correspondingly, the uncertainties on the dipole from the CMB signal are larger than those from the instrument noise.

The uncertainties from *both* are reduced by lowering the Galactic plane cut. In the 15–20 bin of Figure 2 (and to a lesser extent in the 10–15 and 25–30 bins) we see a directional and spectral behavior consistent with a common spatial origin and a CMB spectra (no frequency dependence of the angular deviation). This suggests that large-scale power of the CMB signal is responsible for these displacements (rather than Galactic emission), and that a smaller (not a larger) cut is called for. This is further supported by the fact that for $|b| \gtrsim 20°$, the combined free-free and dust emission from the Galaxy at 53 and 90 GHz produces only ∼10 μK rms (Kogut et al. 1996a), while the CMB signal rms is ∼35 μK (Banday et al. 1996).

To estimate the uncertainty in the dipole results due to the CMB signal we simulate $n = 1.2$, $Q_{\mathrm{rms\text{-}PS}} = 15.3\ \mu\mathrm{K}$ CMB skies for $2 \leq l \leq 25$. We superimpose these maps on a known dipole and solve for the dipole using a 15° Galactic plane cut. No bias is detected and the root mean squares of the results around the input values are 3.3 μK in amplitude, 0°.127 in longitude, and 0°.062 in latitude. We include these uncertainties in the combined systematics.

Galactic cuts greater than 15° are not useful corrections that eliminate more and more Galactic contamination; they introduce systematic errors associated with large Galactic cuts due to the increasingly nonorthogonal basis functions $Y_{lm}(\theta, \phi)$, over the increasingly limited and thus noisier input data. For example, simulations with a 25° cut yield rms uncertainties due to the CMB signal ∼75% larger than the 15° simulations. We conclude that, for the method used here, the Galactic cuts of 10° and 15° are the best compromise to minimize the combined effect of CMB aliasing, Galactic contamination, and noise. The high precision of our dipole direction results depend on this conclusion. Note that this choice for the optimal Galactic cut is smaller than the ≈20° cut used when one is trying to compute the correlation function or determine the $l \geq 2$ components of the power spectrum of the CMB signal, which are smaller than the dipole by a factor of ∼200. For such determinations,

© American Astronomical Society • Provided by the NASA Astrophysics Data System

1996ApJ...470...38L

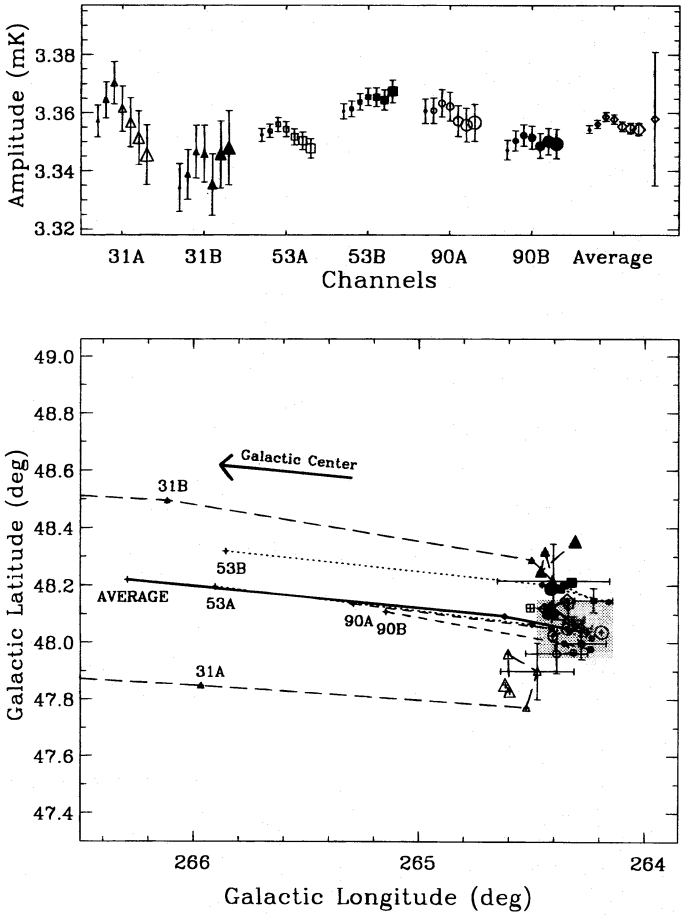

FIG. 1.—Dipole amplitudes (*top*) and directions (*bottom*). The results for each channel and Galactic plane cut (from left to right in the top panel), $|b| > 0°$, 5°, 10°, 15°, 20°, 25°, and 30°, are shown. Channels and cuts are denoted with the same point type and size in both panels. Solutions for the dipole, where no effort has been made to eliminate Galactic emission (i.e., 0° Galactic cuts), are labeled with the channel names 53A, 53B, 90A, and 90B. The 31 GHz labels indicate the 5° cut solutions since their 0° cut solutions are off the plot at longitude $\approx 271°$. For each channel, the successive Galactic cuts are connected by lines (31, *long-dashed lines*; 53, *dotted lines*; 90, *short-dashed lines*; average, *solid line*). The direction of the Galactic center is toward higher latitudes for the same reason that one flies northwest from London to arrive at New York. The latitude and longitude ranges were chosen to display an approximately square piece of the sky. For each channel, the direction error bars on the 15° Galactic cut solutions are shown. Our final dipole amplitude, including the calibration uncertainty is the point in the far right of the top panel. The gray box in the bottom panel denotes the 68% confidence levels of our final dipole direction.

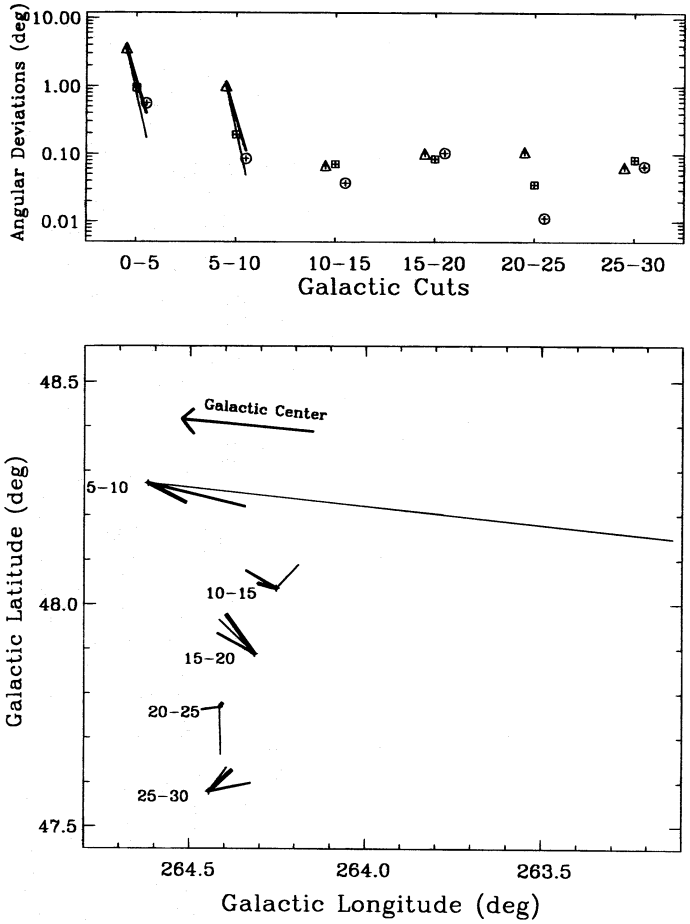

FIG. 2.—Spectral analysis of the angular deviations of the dipole. The vectors of the angular separations between the points in Fig. 1 are indicated here in the bottom panel, while their sizes are plotted in the top panel. The A and B channels at each frequency, 31.5, 53, and 90, have been averaged and are represented, respectively, by triangles, squares, and circles (*top*) and by thin, medium, and thick lines (*bottom*). In the bottom panel, for ease of comparison, the three vectors in a given bin originate at the same point. The 0–5 bin is not shown because it is similar to the 5–10 bin but (as indicated in the top panel) the vectors are approximately 5 times longer. In the top panel, the two reference lines originating on the 31 GHz point of the 0–5 and 5–10 bins indicate the expected spectral behavior if the Galactic emission is pure synchrotron (*thin lines*) and pure free-free (*thick lines*). The points chosen as the common origin of the vectors for each bin are the directions of the channel averages at the smaller of the cuts in each bin pair. The origin latitudes have been offset by 0°.18 with respect to each other to avoid confusion.

the similar compromise for simultaneously minimizing Galactic contamination, instrument noise, and other procedural/systematic effects demands a larger cut.

Our results are averages of the 10° and 15° cuts. We adopt the difference between these two solutions as the 1 σ uncertainty related to this Galactic plane cut choice. We include this uncertainty in the combined systematics, along with the error associated with the aliasing of the CMB signal and the method difference errors mentioned earlier. In general, CMB aliasing is the dominant contributor to the directional combined systematics.

4. RESULTS

Table 1 lists the weighted average of the 10° and 15° Galactic cut results and the uncertainties for each channel. Taking the weighted average of all six channels we obtain a best-fit dipole amplitude $3.358 \pm 0.001 \pm 0.023$ mK in the direction $(l, b) = (264°.31 \pm 0°.04 \pm 0°.16, +48°.05 \pm 0°.02 \pm 0°.09)$, where the first uncertainties are statistical and the second are estimations of the combined systematics. In celestial coordinates the direction is $(\alpha, \delta) = (11^h11^m57^s \pm 23^s, -7°.22 \pm 0°.08)$ (J2000). The uncertainty in the dipole amplitude is dominated by the absolute calibration of the DMR instrument (Kogut et al. 1996b). This is easily seen in Figure 1 by comparing the large error bars on our final result (*far right*) with the noise-only error bars on the channel results. The calibration uncertainty plays no role in the directional uncertainty for the same reason that the directions of vectors $\boldsymbol{x}$ and $a\boldsymbol{x}$ (where a is any positive constant) are the same. The uncertainty in the direction is dominated by the combined systematic effects discussed above.

Under the assumption that the Doppler effect is responsible for the entire CMB dipole, the velocity of the

© American Astronomical Society • Provided by the NASA Astrophysics Data System

1996ApJ...470...38L

TABLE 1

CHANNEL DIPOLE RESULTS

Channel	Amplitude (μK)[a]	Galactic Longitude (deg)	Galactic Latitude (deg)
31A			
Mean	3366	264.50	47.83
Total error	85	0.22	0.23
Noise	7	0.14	0.09
Calibration[b]	84	0.00	0.00
Combined systematics	10	0.16	0.21
31B			
Mean	3346	264.46	48.25
Total error	77	0.30	0.24
Noise	9	0.23	0.12
Calibration[b]	76	0.00	0.00
Combined systematics	4	0.20	0.20
53A			
Mean	3355	264.28	48.05
Total error	23	0.18	0.10
Noise	2	0.07	0.03
Calibration[b]	23	0.00	0.00
Combined systematics	4	0.17	0.09
53B			
Mean	3364	264.19	48.15
Total error	24	0.17	0.08
Noise	2	0.08	0.04
Calibration[b]	23	0.00	0.00
Combined systematics	4	0.15	0.07
90A			
Mean	3362	264.35	47.96
Total error	67	0.20	0.11
Noise	4	0.13	0.07
Calibration[b]	67	0.00	0.00
Combined systematics	3	0.15	0.09
90B			
Mean	3351	264.26	47.99
Total error	43	0.17	0.09
Noise	3	0.10	0.05
Calibration[b]	43	0.00	0.00
Combined systematics	3	0.14	0.07
Total			
Mean	3358	264.31	48.05
Total error	23	0.17	0.10
Noise	1	0.04	0.02
Calibration[b]	23	0.00	0.00
Combined systematics	4	0.16	0.09

[a] Values are in thermodynamic temperature transformed from antenna temperature by $\Delta T = \Delta T_{ant}(e^x - 1)^2/x^2e^x$, where $x = h\nu/kT_0$, $T_0 = 2.73$ K. The conversion factors are thus 1.026, 1.074, and 1.227 for 31.5, 53, and 90 GHz, respectively.

[b] See Table 2 of Kogut et al. 1996b for absolute calibration uncertainties.

Sun with respect to the rest frame of the CMB is $v_\odot = 369.0 \pm 2.5$ km s^{-1}, which corresponds to the dimensionless velocity $\beta = v_\odot/c = 1.231 \pm 0.008 \times 10^{-3}$. The associated rms Doppler quadrupole[8] is $Q_{rms} = 1.23 \pm 0.02$ μK with components $[Q_1, Q_2, Q_3, Q_4, Q_5] = [0.91 \pm 0.02, -0.20 \pm 0.01, -2.05 \pm 0.03, -0.91 \pm 0.02, 0.18 \pm 0.01]$ μK.

5. SUMMARY AND DISCUSSION

We have used the DMR 4 year data set to obtain a best-fit CMB dipole amplitude 3.358 ± 0.023 mK and direction $(l, b) = (264.^\circ31 \pm 0.^\circ17, +48.^\circ05 \pm 0.^\circ10)$. Figure 3 displays the main results of this paper and compares them with other *COBE* results: the DMR first year (Kogut et al.

© American Astronomical Society • Provided by the NASA Astrophysics Data System

1996ApJ...470...38L

1993), the DMR first 2 years (Bennett et al. 1994), the FIRAS (Fixsen et al. 1994, 1996) dipole results, and a pixel-based likelihood analysis of the DMR 4 year data (Bennett et al. 1996).

Although the results are consistent, our independent analysis differs from the Bennett et al. (1996) analysis in many detailed ways. The most important difference is our strategy for removing the Galactic foreground; we have examined the dipole results as a function of Galactic plane cut and frequency and find that Galactic contamination of the dipole is not important for Galactic cuts as low as 10° or 15°. The largest source of directional error, aliasing of CMB power combined with instrument noise, can be reduced by using these smaller Galactic plane cuts. The result is substantially smaller errors on the dipole direction.

The good agreement of the DMR and FIRAS dipole results is further evidence that the systematic uncertainties of these two *COBE* instruments are fairly well understood.

We acknowledge the constructive comments of the anonymous referee. We also gratefully acknowledge NASA for funding the *COBE* satellite and data processing and the many people responsible for the high quality of the *COBE* DMR data. C. H. L. acknowledges support from the French Ministère des Affaires Etrangères. L. T. was partially supported by grants DGICYT PB94-0364 and DMS-9404276.

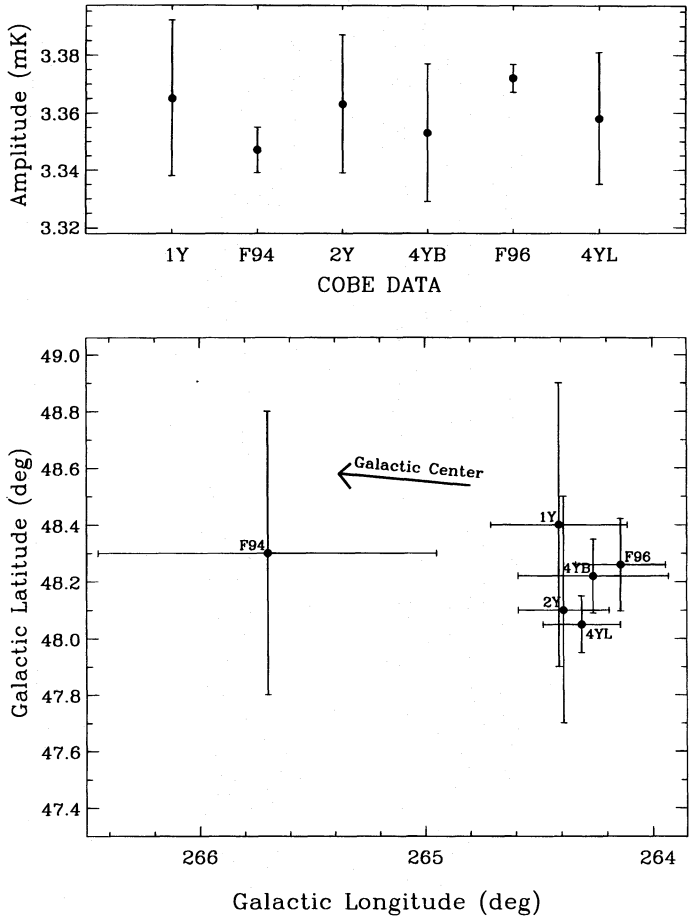

FIG. 3.—*COBE* dipoles. The DMR dipole results: 1Y, Kogut et al. (1993); 2Y, Bennett et al. (1994); 4YB, Bennett et al. (1996); and 4YL, this work, are consistent with each other and with the FIRAS results F94, F96 (Fixsen et al. 1994, 1996). We have adjusted the published FIRAS error bars to include CMB aliasing using the 15° cut simulation results (§ 3.2).

[8] $Q_{\rm rms}^2 = \frac{4}{15}[\frac{3}{4}Q_1^2 + Q_2^2 + Q_3^2 + Q_4^2 + Q_5^2]$, where the components are defined by $T_0\beta^2/2[2\cos^2\theta - (2/3)] = Q_1(3\sin^2 b - 1)/2 + Q_2 \sin 2b \cos l + Q_3 \sin 2b \sin l + Q_4 \cos^2 b \cos 2l + Q_5 \cos^2 b \sin 2l$, where T_0 is the mean CMB temperature and θ is the angle between the dipole direction and the direction of observation: (l, b).

REFERENCES

Banday, A. J., et al. 1996, ApJ, in press
Bennett, C. L., et al. 1994, ApJ, 436, 423
———. 1996, ApJ, 464, L1
Bersanelli, M., et al. 1996, A&AS, in press
Fixsen, D. J., et al. 1994, ApJ, 420, 445
———. 1996, ApJ, 470, in press
Kogut, A., et al. 1993, ApJ, 419, 1
———. 1996a, ApJ, 464, L5
———. 1996b, ApJ, 470, in press
Lineweaver, C. H., et al. 1995, Astrophys. Lett. Comm., 32, 173
Smoot, G. F., et al. 1991, ApJ, 371, L1
Wright, E. L., et al. 1994, ApJ, 420, 1

© American Astronomical Society • Provided by the NASA Astrophysics Data System